

Electronic Supplementary Information

**Carbon fibre paper coated by a layered manganese oxide: a  
nano-structured electrocatalyst for water-oxidation with  
high activity over a very wide pH range**

Jens Melder,<sup>a</sup> Stefan Mebs,<sup>b</sup> Philipp A. Heizmann,<sup>a</sup> Rebekka Lang,<sup>a</sup>  
Holger Dau<sup>\*b</sup> and Philipp Kurz<sup>\*a</sup>

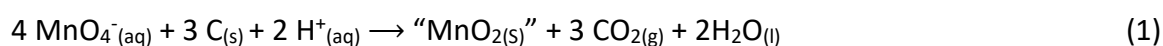
<sup>a</sup>Institut für Anorganische und Analytische Chemie and Freiburger Materialforschungszentrum (FMF), Albert-Ludwigs-Universität Freiburg, Albertstraße 21, 79104 Freiburg (Germany)

<sup>b</sup>Fachbereich Physik, Freie Universität Berlin, Arnimallee 14, 14195 Berlin

## Materials and Methods:

All reagents and solvents were purchased from commercial sources and, unless otherwise stated, used without further purification. For the preparation of the potassium phosphate buffer and the stock solutions for fAAS measurements ultra-pure water (ELGA PURELAB flex) was used. All other experiments were carried out in deionised water. All data was processed with the OriginPro 2018G software package, unless otherwise stated.

**Electrode Preparation** The coating of binder free MnO<sub>x</sub> on graphitized carbon fiber paper was achieved via an in-situ redox deposition approach between the carbon support and an acidic (pH~0.4, 2.5 mL HNO<sub>3</sub> (69 %)) 0.1 M potassium permanganate solution (100 mL) following Equation (1).



First, the strongly acidic mixture was heated to 70 °C and subsequently four pretreated CFP supports were dipped into the stirred solution simultaneously. To ensure that only 1 cm<sup>2</sup> of the carbon material was exposed to the solution, the rest of the area was covered with adhesive tape (tesafilm<sup>®</sup>, "matt-unsichtbar", thickness ~70 μm). This step was carried out for different times (15 - 360 min) in order to obtain different thicknesses of the MnO<sub>x</sub> layer. A schematic representation of the functionalization setup and images of electrodes before and after redox-deposition can be found in Figure S19. The electrodes were then taken out of the KMnO<sub>4</sub> solution, washed thoroughly with water, dried in air at 60°C for 1 h and finally calcined in a muffle furnace in air at a temperature of 400°C for 1 h.

The reduction of manganese from acidic KMnO<sub>4</sub> solutions leads to the formation of layered manganese oxides containing intercalated H<sup>+</sup>/K<sup>+</sup> ions. The precise looking Equation (1) is only a simplification and the acidic birnessite has a more complex composition as "MnO<sub>2</sub>" (see main text). Furthermore, in addition to CO<sub>2</sub> carbon is known to also form so-called "surface oxides" (-COOH, -COH, -CO) at strongly oxidizing conditions. Therefore, no pronounced CO<sub>2</sub> gas evolution was observed during the deposition process; thus, the decoration of the carbon supports by "surface oxides" seems to be an important process. Furthermore, such surface oxides could serve as anchor for the metal oxide. For more information on the preparation see Ref.<sup>[1]</sup>

**ATR-FT-IR-spectroscopy** IR spectra of the MnO<sub>x</sub>/C-electrodes before and after electrochemical long-term treatment were carried out with a Nicolet 13 iS10 FT-IR spectrometer (Thermo Fisher Scientific) equipped with a diamond ATR-unit. All ATR-IR spectra were baseline corrected and recorded in the spectral range from 4000-450 cm<sup>-1</sup>.

**Raman-spectroscopy** Raman spectra were recorded with a WiTec alpha500 AR Raman microscope. The excitation source is a laser with a wavelength of 532 nm, which is obtained using a frequency doubled Nd:YAG laser with an maximum excitation power of around 17 mW. A CCD detector, thermoelectrically cooled to -67°C, was employed in the measurement set-up. All Raman spectra were recorded at 20-times magnification and

maximum laser power. Every spectrum is the result of the overlay of 30 individual spectra obtained for an integration time of 2 s. Raw spectra were baseline-corrected and deconvoluted using a sum of Lorentzian functions by means of an unconstrained non-linear Lavenberg-Marquardt optimization algorithm implemented in the OriginPro 2018G software package.

**Scanning electron microscopy and energy dispersive X-ray analysis (SEM and EDX)** SEM was performed using a FEG-SEM SU8220 (Hitachi) equipped with a secondary electron in-lens detector and four Bruker silicon drift detectors (sdd) for EDX analysis. The images were taken in a distance of approximately 8 mm with an acceleration voltage of 12 kV. EDX analyses were performed at a distance of 15 mm and acceleration voltages of 15 kV.

**Grazing incidence powder X-ray diffractometry (GI-XRD)** GI-XRD patterns of MnO<sub>x</sub>/C-electrodes and carbon substrates were recorded in reflection geometry with a Seifert 3003 TT diffractometer and Cu-K $\alpha$ -radiation ( $\lambda = 0.154060$  nm). The electrodes were therefore mounted on a Plexiglas holder. Data were collected over  $2\theta$  angles from 10 to 80°.

**Flame atomic absorption spectroscopy (fAAS)** Concentrations of manganese and potassium ions were determined with a F-AAS novAA350 (Analytik Jena). A solution of HNO<sub>3</sub> (1%, w/w) served as diluent and the F-AAS was calibrated with K- and Mn(II)-nitrate standard solutions (Roth). Prior to analysis, the MnO<sub>x</sub>/CFP electrodes were treated with 0.1 mL of a 1 : 10-mixture of concentrated HNO<sub>3</sub> and 30% H<sub>2</sub>O<sub>2</sub>, which completely dissolved the oxide from the carbon support and converted all manganese to its Mn<sup>2+</sup> form. The solutions were then diluted to 25 mL. Electrolytes (50 mL) were directly measured without any further dilution.

**XANES and EXAFS** were conducted at the KMC3 beamline of the BESSY synchrotron operated at the Helmholtz-Zentrum Berlin (HZB). Data collection was performed at 20 K in a liquid-helium cryostat in fluorescence detection mode using a 13 element ultra-low energy resolving Ge detector (Canberra). Over 20 spectra were averaged for each compound in order to improve the signal-to-noise ratio. Averaged spectra were background-corrected and normalized using in-house software. Subsequently, unfiltered  $k^3$ -weighted spectra and phase functions from FEFF8.5<sup>[2]</sup> were used for least-squares curve-fitting of the EXAFS with in-house software and for calculation of Fourier-transforms representing  $k$ -values between 1.6 and 14 Å<sup>-1</sup>. Data were multiplied by a fractional cosine window (10% at low and high  $k$ -side); the amplitude reduction factor  $S_0^2$  was 0.7.

**Preparation of K-phosphate buffer solutions** Potassium phosphate buffer solutions with different pH and different concentrations were prepared from concentrated phosphoric acid (85%, ACS quality) by dilution with ultra-pure water. The pH was adjusted by adding KOH pellets (ACS quality). All pH measurements were carried out with an inolab ids 9310 pH-meter from WTW equipped with a SenTix980 pH electrode.

## **Electrochemistry:**

**Electrochemical multi-step protocol** To evaluate the electrocatalytic behavior of the  $\text{MnO}_x/\text{C}$ -electrodes a multi-step protocol was used. EIS measurements for the determination of the uncompensated resistance were performed at the open circuit potential (OCP) by applying an AC voltage with an amplitude of  $10 \text{ mV}_{\text{RMS}}$  in a frequency range of 100 kHz to 10 Hz. For the determination of Tafel-plots a staircase type chronoamperometry program in which the potential of the working electrode was increased stepwise from 1.22 to 2.02 V vs. RHE was used. At each step the potential was held constant for 300 s (5 min). To calculate the Tafel-plots the average over the last 30 s of the current-density  $j$  at the end of each upward staircase was calculated. Cyclic voltammograms were recorded for the range of 0.82-2.02 V vs RHE with a scan rate of  $20 \text{ mV s}^{-1}$ .

**Electrochemical impedance spectroscopy (EIS)** The electrochemical impedance spectroscopy measurements for the determination of the electrolyte resistances were performed at the open circuit potential (OCP) by applying an AC voltage with an amplitude of 10 mV in a frequency range of 100 kHz to 1 Hz. EIS data were analyzed with the ZView software package from Scribner Associates. For the simulation of the EIS data, an equivalent circuit based on a simple Randles cell was used. The double-layer capacitance was modelled as a constant phase element owing to the porous structure of the electrode.

**In-operando UV/Vis spectroscopy** In operando UV/Vis spectroscopy measurements of the electrolytes during electrochemical chronoamperometry experiments at different potentials were conducted with a Varian Cary 50 Conc UV/Vis spectrophotometer equipped with a dip probe accessory which was placed directly in front of the  $\text{MnO}_x$  working electrode. The counter electrode was placed in a compartment separated by a porous glass frit to exclude the reduction of any oxidatively generated by-products, e.g.  $\text{MnO}_4^-$ . All spectra were baseline corrected and measured in the range from 400-800 nm with a scan speed of  $20 \text{ nm min}^{-1}$ .

## Additional Figures:

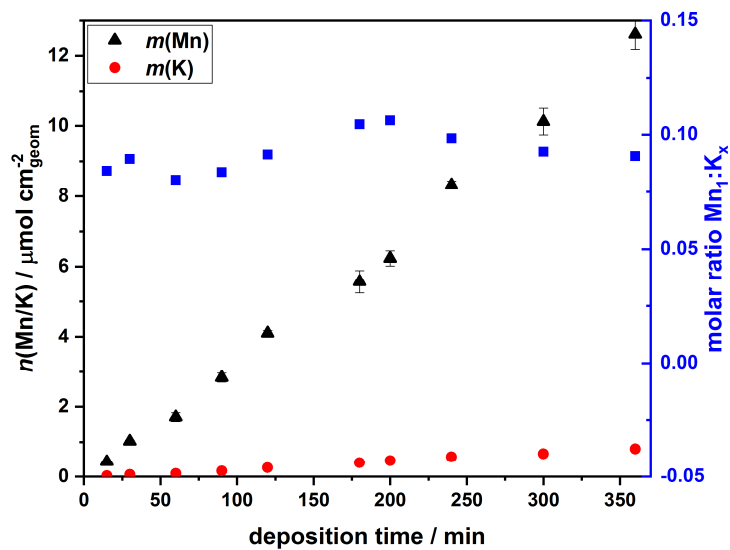


Figure S1. dependence of the deposition time and the deposited amount of Mn (black triangle) and K (red dots) per geometric surface area of MnO<sub>x</sub>/CFP-electrodes; molar Mn:K ratio normalized to the number of Mn atoms (blue squares).

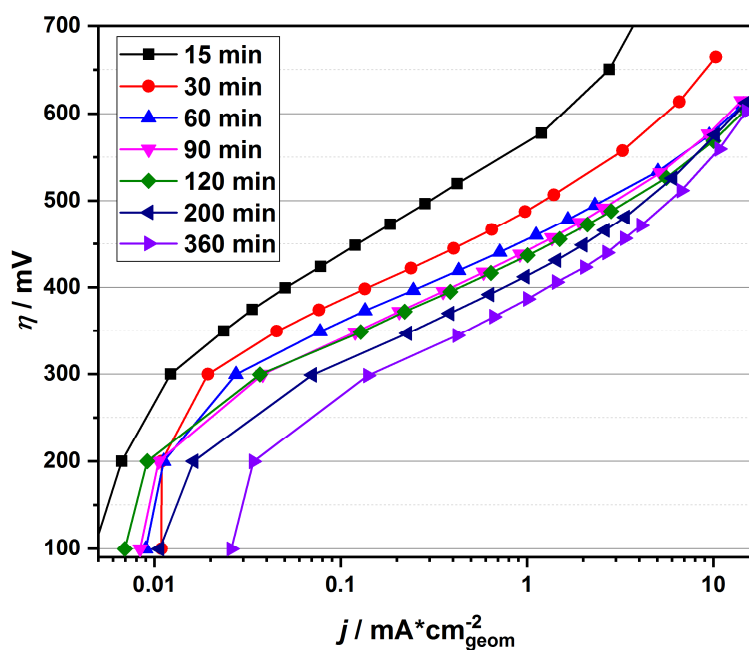


Figure S2. Tafel plots of MnO<sub>x</sub>/CFP-electrodes functionalized for different times normalized to the geometric area; extracted from stepwise chronoamperometry measurements.

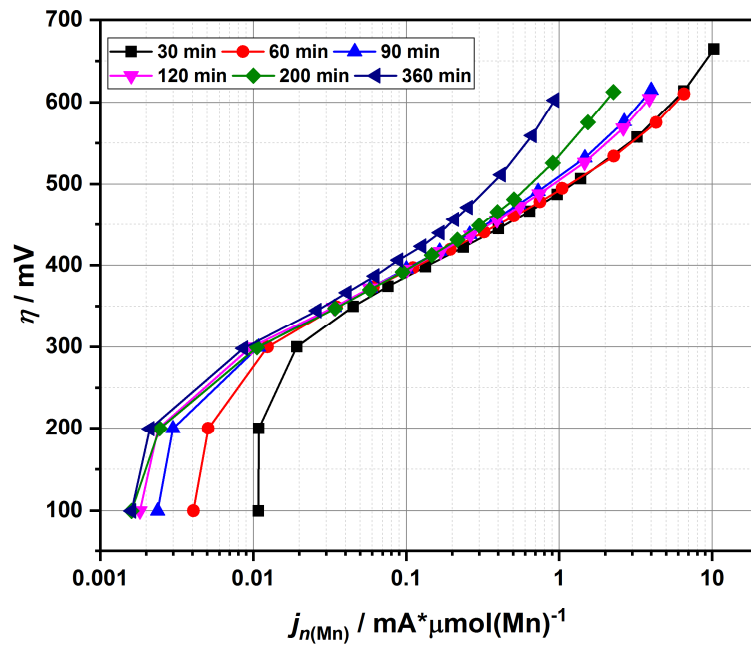


Figure S3. Tafel plots of MnO<sub>x</sub>/CFP-electrodes functionalized for different times normalized to the number of deposited Mn-ions area; extracted from stepwise chronoamperometry measurements.

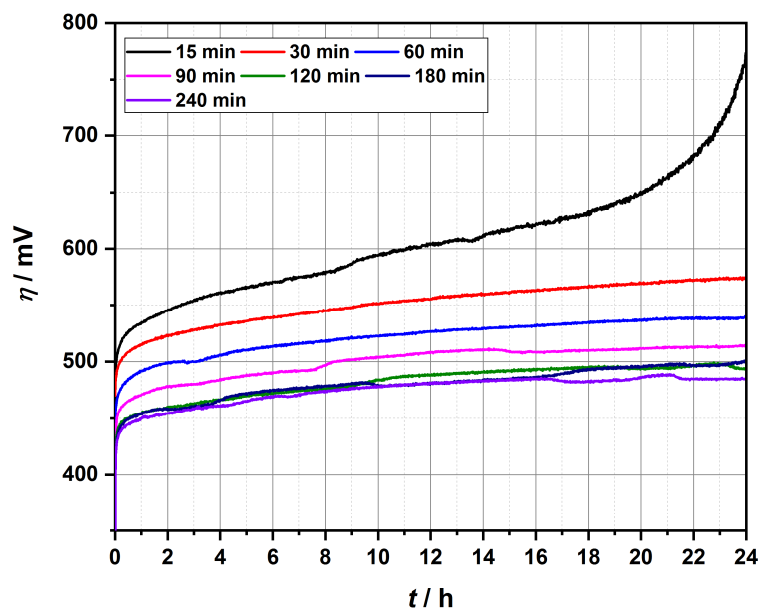


Figure S4. long-term chronopotentiometric measurements of MnO<sub>x</sub>/CFP functionalized for different times; conditions: 0.4 M KPi (pH 7),  $j = 2 \text{ mA cm}^{-2}$ .

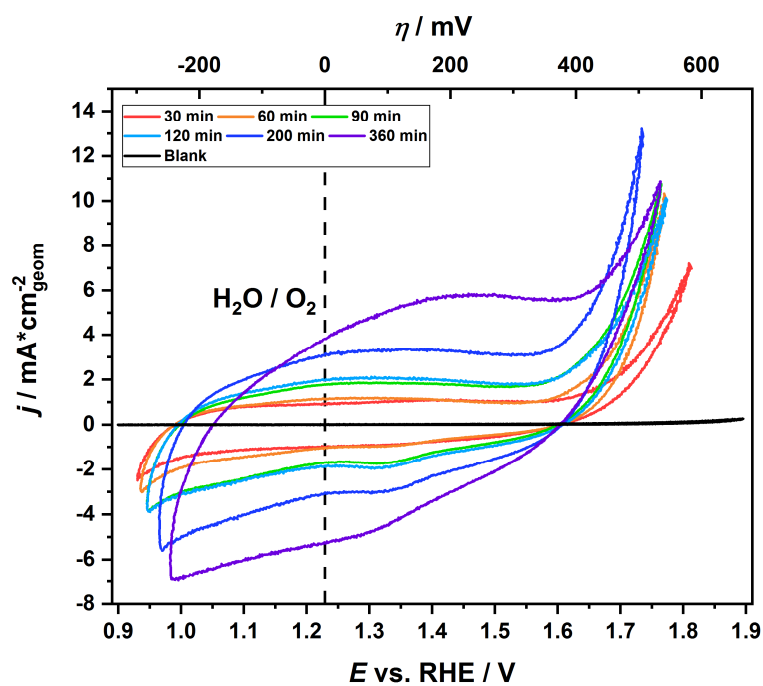


Figure S5. cyclic voltammograms recorded in the potential range from 0.9-1.9 V of  $\text{MnO}_x/\text{CFP}$  functionalized for different times. Conditions: 0.4 M  $\text{KPi}$  (pH 7), scan-rate: 20 mV/s, iR-corrected at 85%.

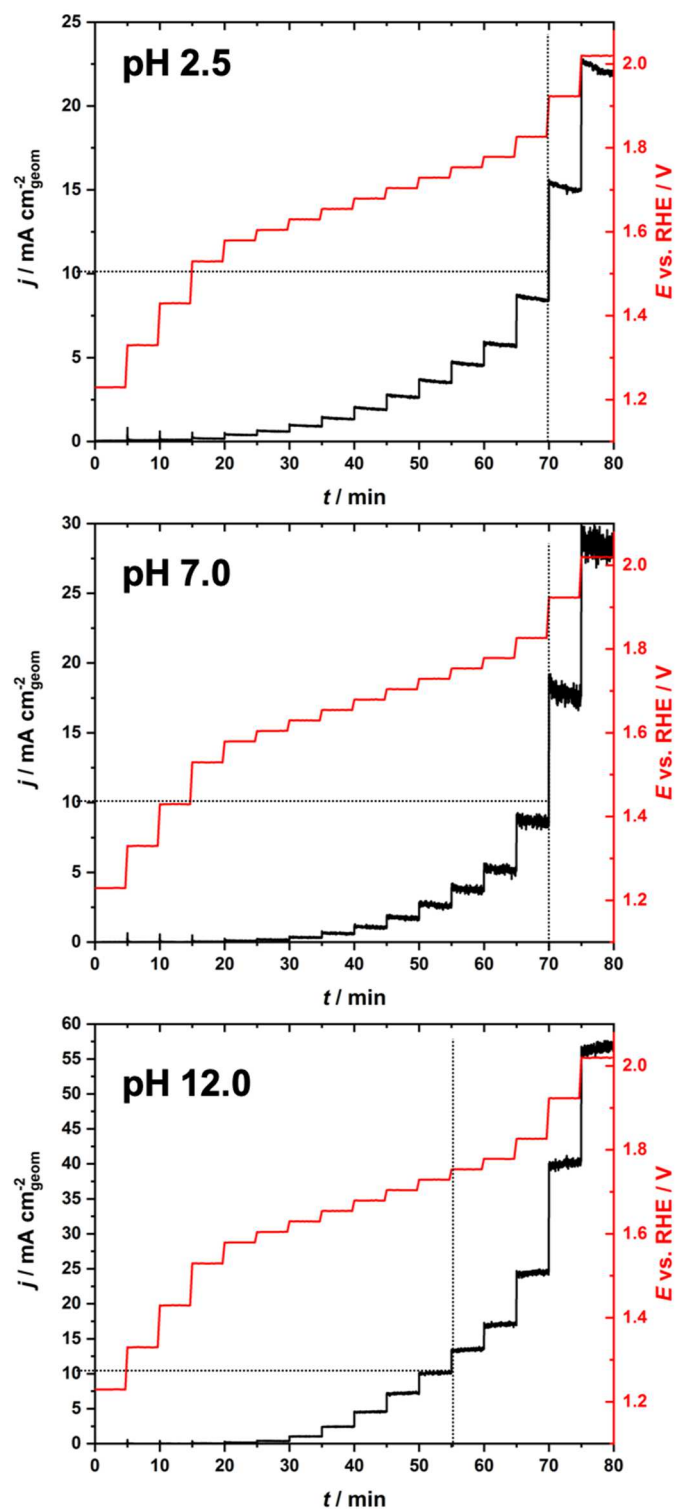


Figure S6. stepwise chronoamperometry measurements for MnO<sub>x</sub>/CFP at pH 2.5/7.0/12.0. The measurements are the basis of the Tafel-plots shown in Fig. 2b of the main text. The steps from which the Tafel-plots were determined are framed by dotted lines.



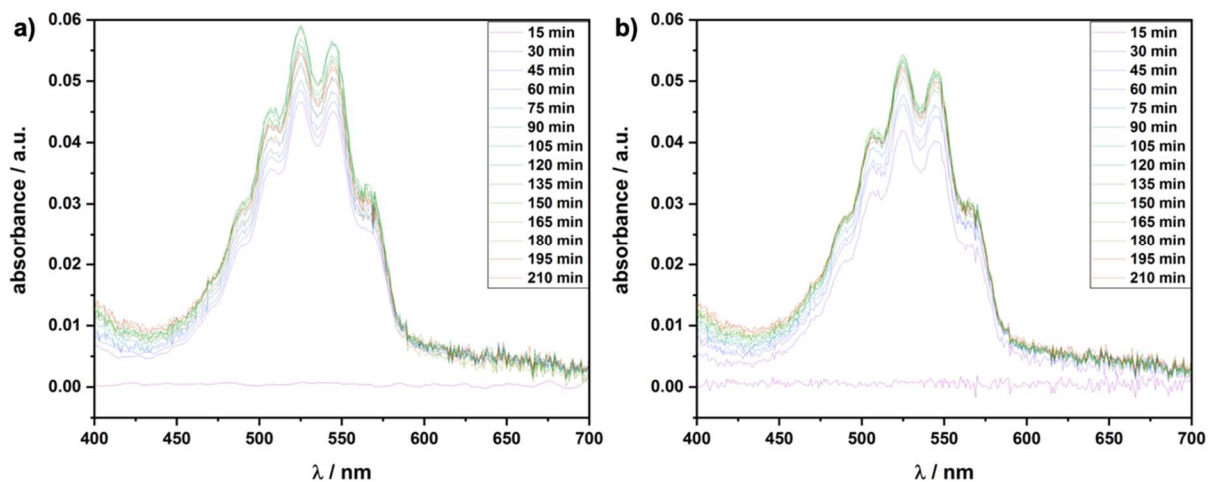


Figure S7. in-operando UV/Vis-absorption spectra of 1 M  $KP_i$ -electrolytes (a) pH 2.5, b) pH 7) during electrolysis of a  $MnO_2/CFP$ -electrode at a constant potential of 1.8 V for 3.5 h.

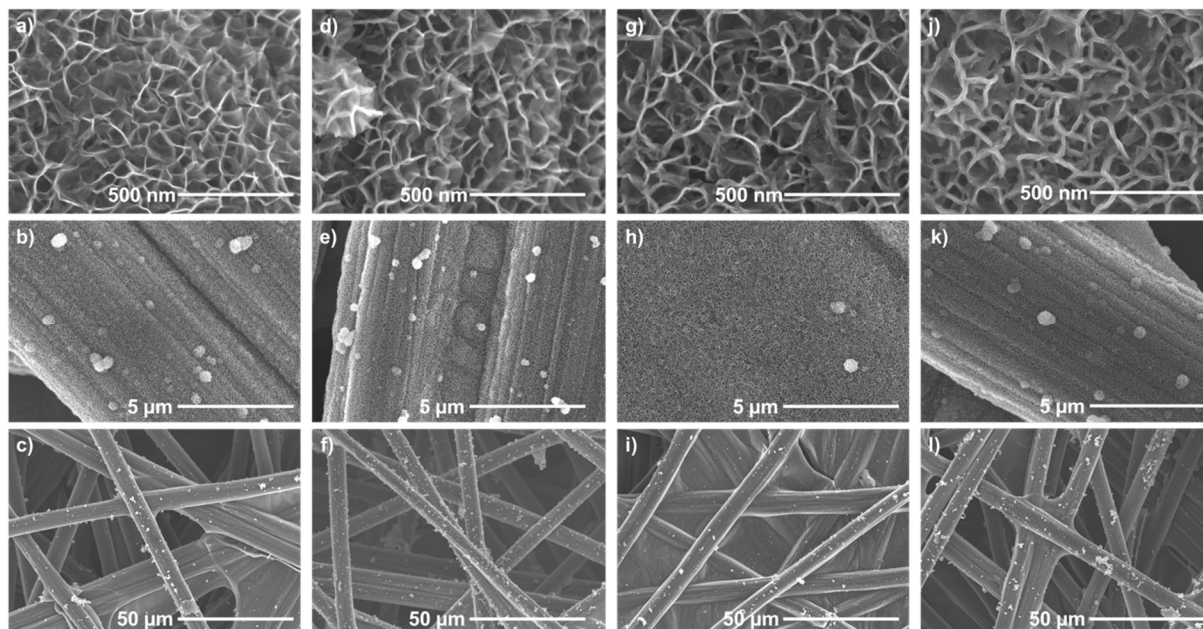


Figure S8. additional SEM micrographs at different magnifications (top row: x100k; middle row: x10k; lower row: x1k) of the as prepared (a-c)  $MnO_2@C$ -electrodes and after chronopotentiometric long-term measurements in 1M  $KP_i$  at a constant current density of  $2 \text{ mA cm}^{-2}$  for 24h at pH 2.5 (d-f), pH 7 (g-i) and pH 12 (j-l).

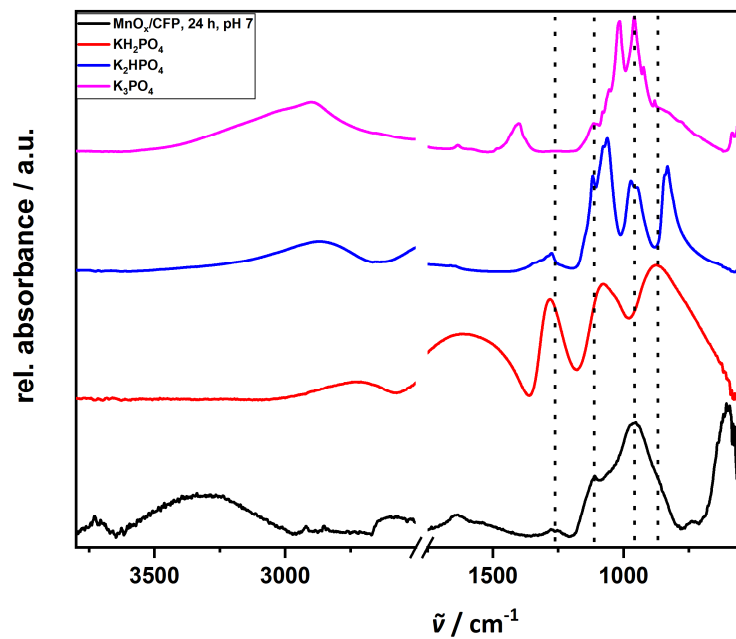


Figure S9. ATR-IR spectra of KH<sub>2</sub>PO<sub>4</sub>, K<sub>2</sub>HPO<sub>4</sub> and K<sub>3</sub>PO<sub>4</sub> in comparison to an MnO<sub>x</sub>/CFP electrode used for 24 h as anode in 1M KP<sub>i</sub> buffer at pH 7.

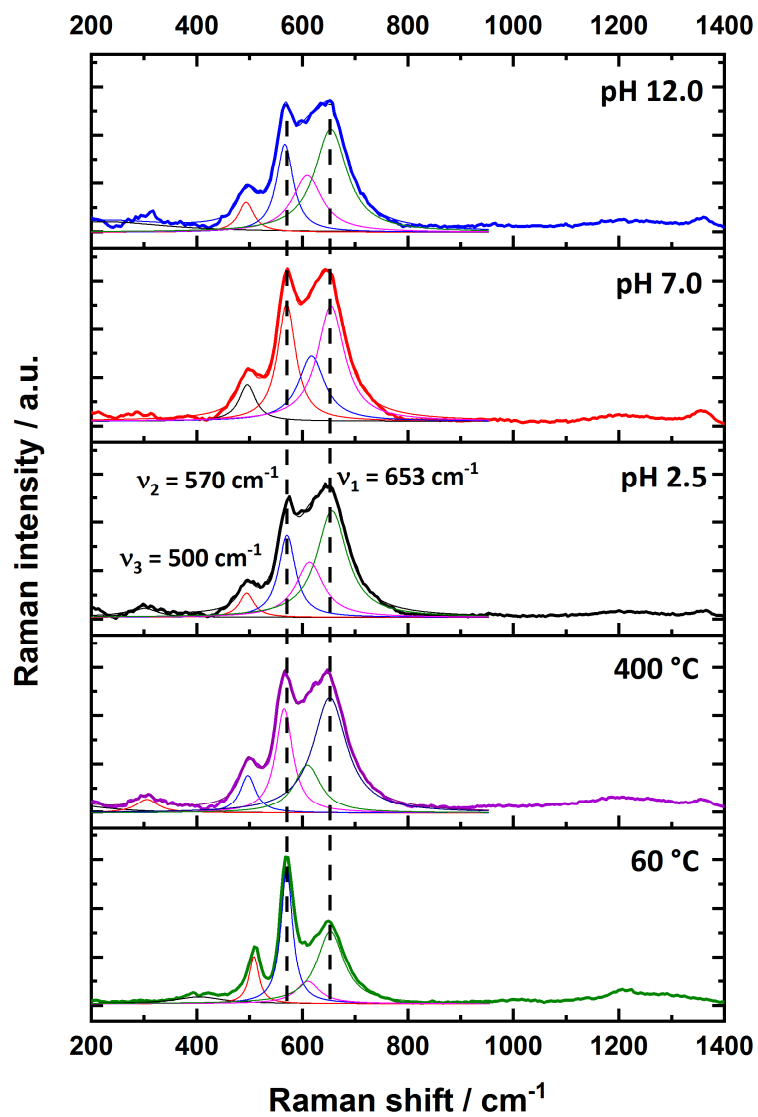


Figure S10. Raman spectra of pristine  $\text{MnO}_x/\text{CFP}$ -electrodes dried at 60 °C and activated at 400 °C and activated electrodes operated for 24h in 1M  $\text{KPi}$ -buffer at a constant current density  $j = 2 \text{ mA}\cdot\text{cm}^{-2}$  and different pH (2.5/7/12).

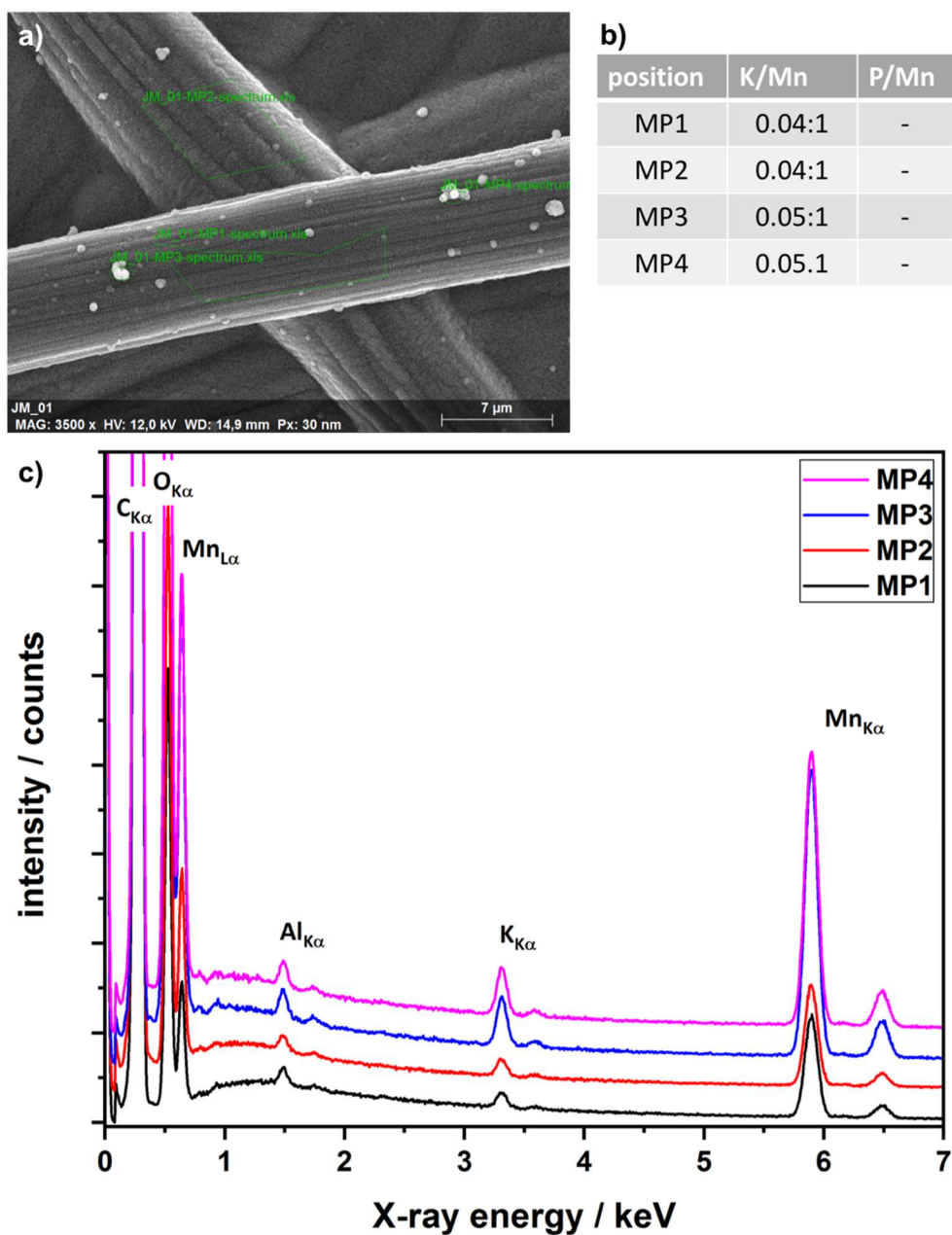


Figure S11. Typical EDX spectra of an as-prepared  $\text{MnO}_x/\text{CFP}$ -electrode (c); the SEM micrograph in a) shows the position where the EDX spectra were recorded; the table (b) shows the molar ratios of K/Mn and P/Mn. The signal from C originates from the catalysts support; signals from Al and Cu are due to the sample holder.

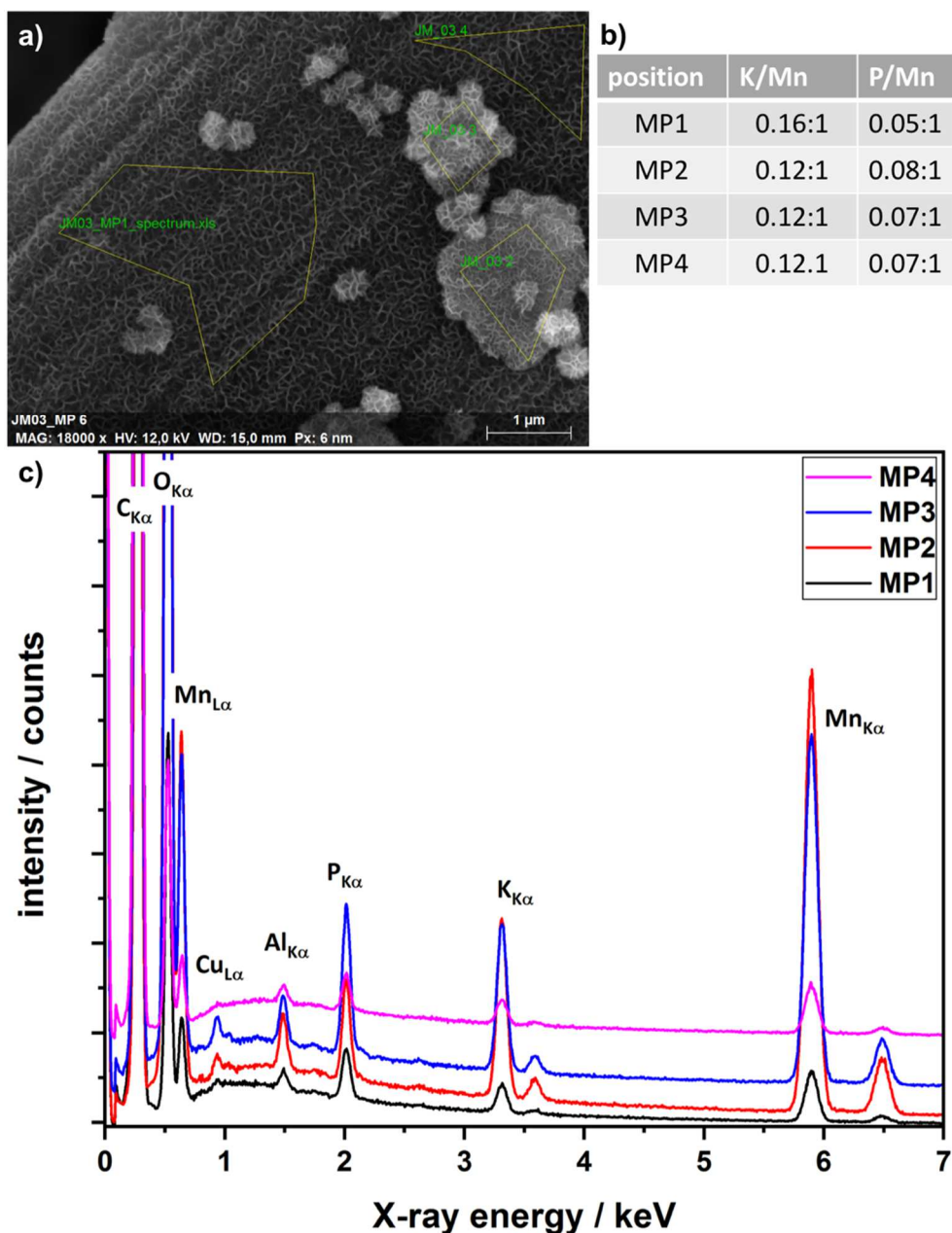


Figure S12. Typical EDX spectra of a  $\text{MnO}_x/\text{CFP}$ -electrode electrochemically tested in 1.0 M  $\text{KP}_i$ -buffer solution (pH 2.5) at a constant current density of  $2 \text{ mA cm}^{-2}$  (c); the SEM micrograph in a) shows the position where the EDX spectra were recorded; the table (b) shows the molar ratios of K/Mn and P/Mn. The signal from C originates from the catalysts support; signals from Al and Cu are due to the sample holder.

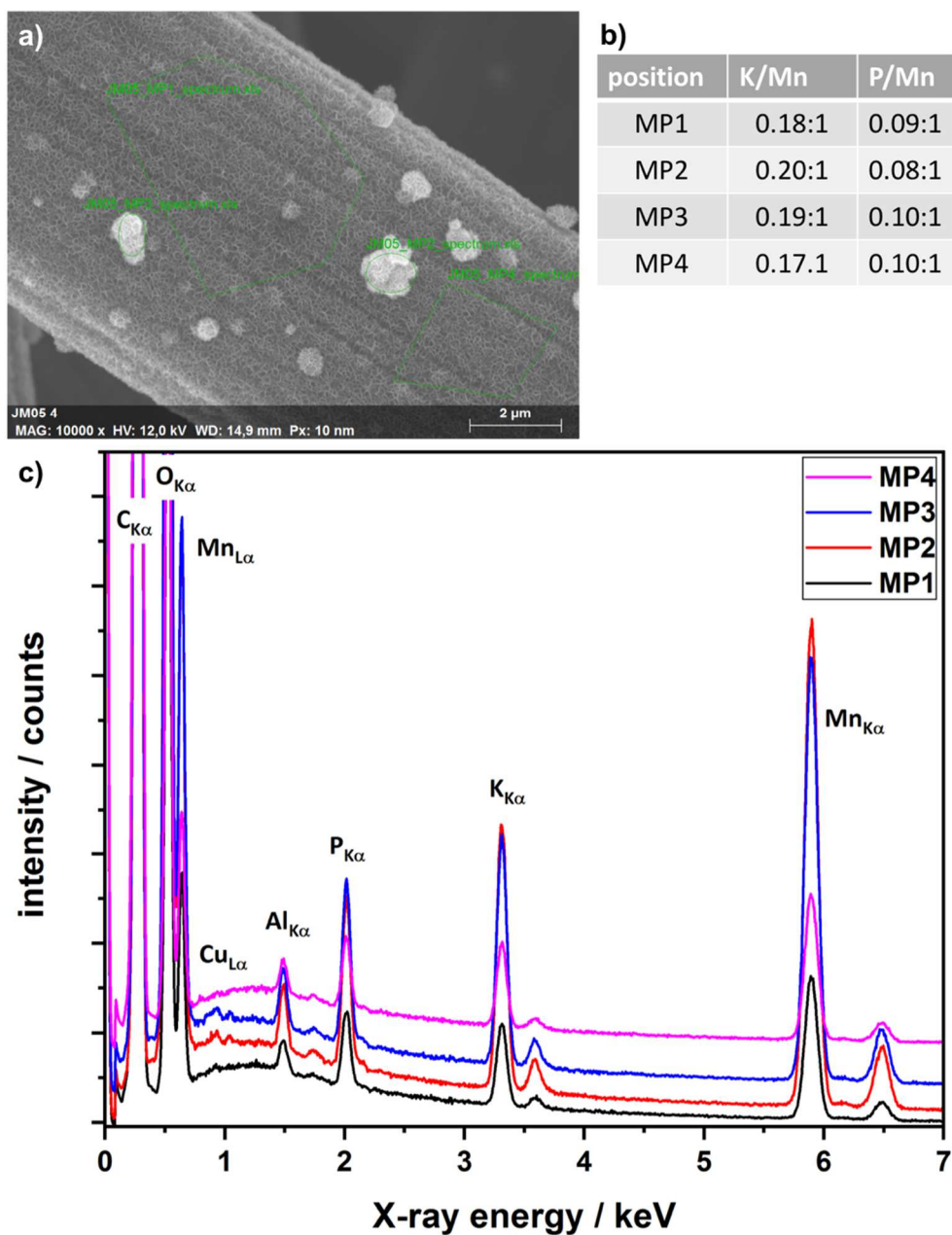


Figure S13. Typical EDX spectra of a  $\text{MnO}_x/\text{CFP}$ -electrode electrochemically tested in 1.0 M  $\text{KPi}$ -buffer solution (pH 7) at a constant current density of  $2 \text{ mA cm}^{-2}$  (c); the SEM micrograph in a) shows the position where the EDX spectra were recorded; the table (b) shows the molar ratios of K/Mn and P/Mn. The signal from C originates from the catalysts support; signals from Al and Cu are due to the sample holder.

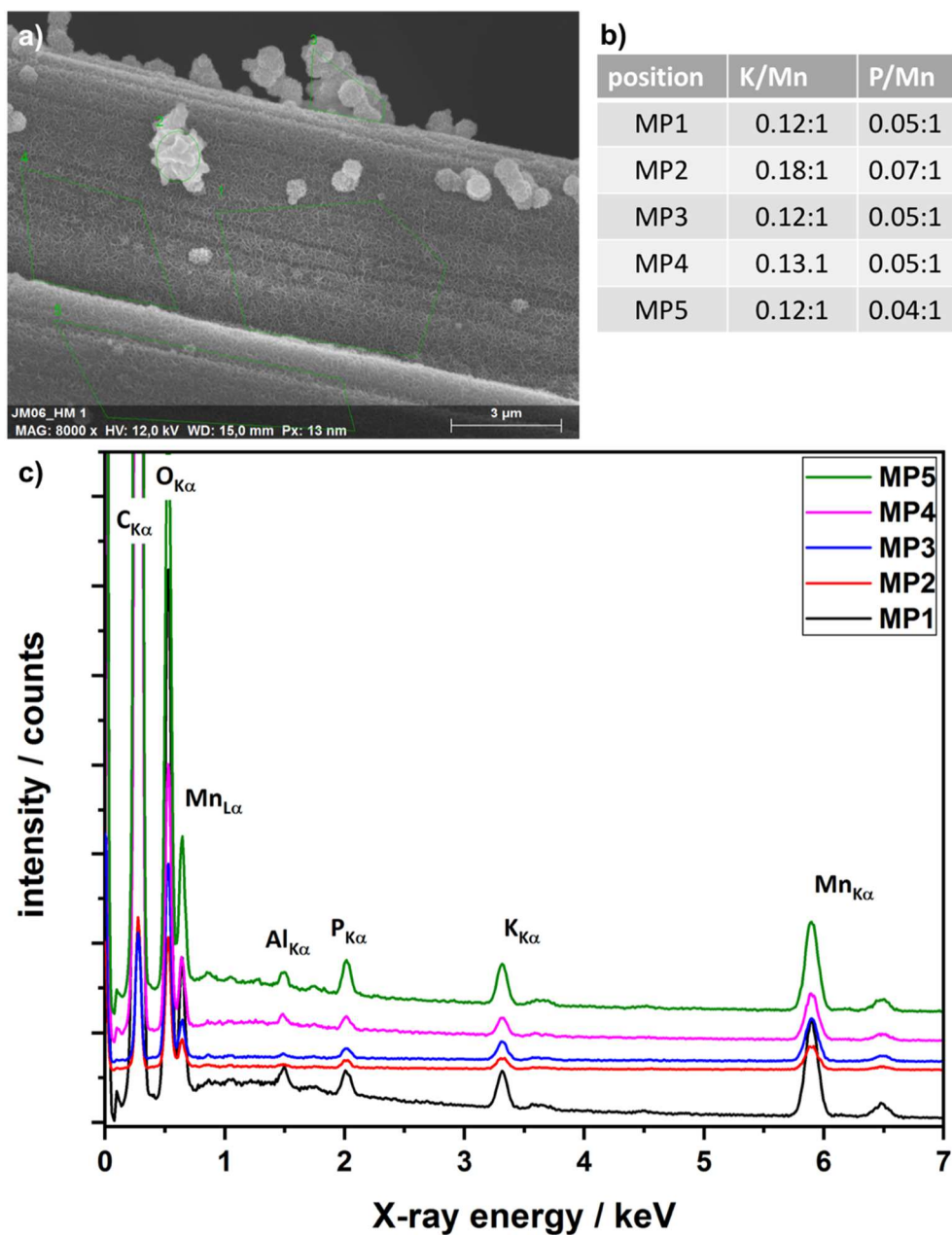


Figure S14. Typical EDX spectra of a  $\text{MnO}_x/\text{CFP}$ -electrode electrochemically tested in 1.0 M  $\text{KPi}$ -buffer solution (pH 12) at a constant current density of  $2 \text{ mA cm}^{-2}$  (c); the SEM micrograph in a) shows the position where the EDX spectra were recorded; the table (b) shows the molar ratios of K/Mn and P/Mn. The signal from C originates from the catalysts support; signals from Al and Cu are due to the sample holder.

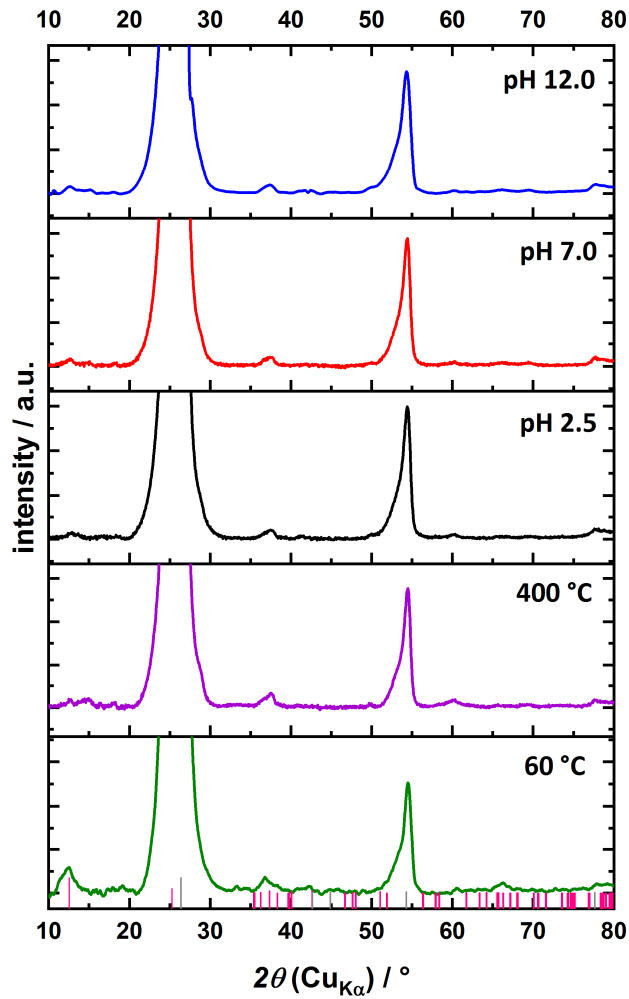


Figure S15. diffraction patterns of  $\text{MnO}_x/\text{CFP}$ -electrodes dried at  $60^\circ\text{C}$  and activated at  $400^\circ\text{C}$  and activated electrodes operated for 24h in 1M  $\text{KP}_i$ -buffer at a constant current density  $j = 2 \text{ mA cm}^{-2}$  at different pH (2.5/7/12). Theoretical reference patterns of graphite<sup>[3]</sup> and K-birnessite<sup>[4]</sup> are shown as bar graphs in grey and pink, respectively.

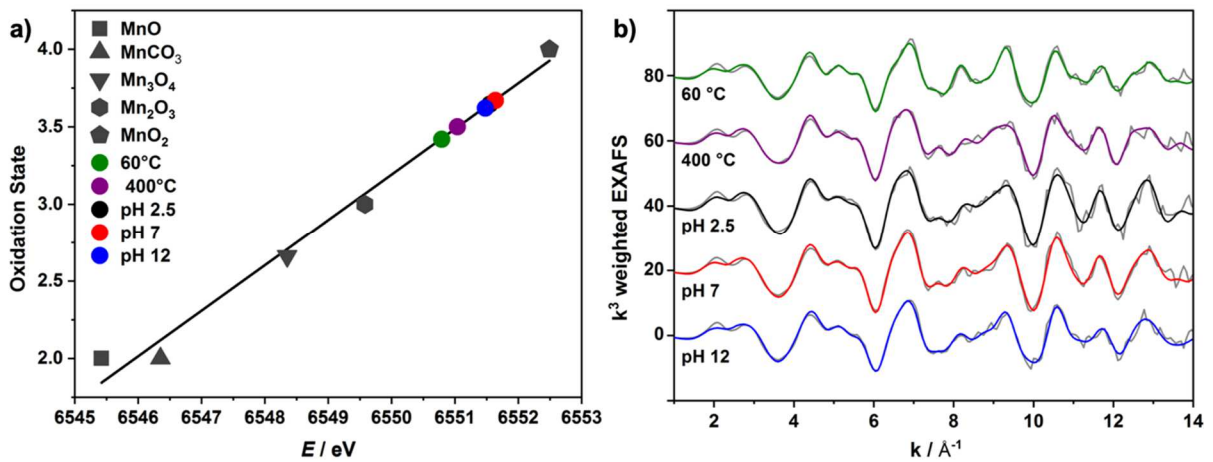


Figure S16. a) Oxidation states of deposited samples derived from a linear fit of the data extracted at a normalized X-ray absorption intensity of 0.5 for reference compounds. b)  $k^3$  weighted EXAFS spectra ( $k^3$  weighted) and respective fits.



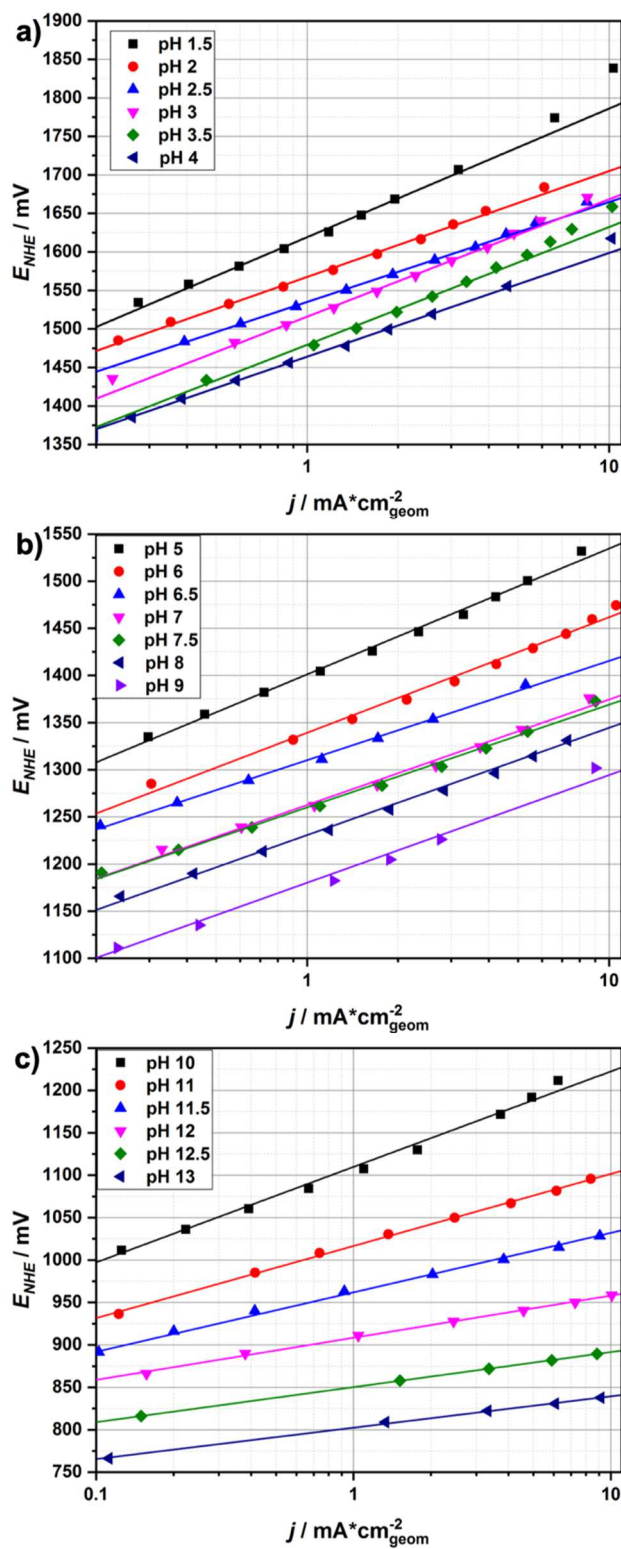


Figure S17. Tafel-plots for  $\text{MnO}_x/\text{CFP}$  in 1 M  $\text{KPi}$  buffer solution at pH 1.5- 4.0 (a), 5.0-9.0 (b) and pH 10.0 -13.0 (c). Please note that instead of the overpotential  $\eta$  the potential  $E_{NHE}$  with respect to the pH dependent normal hydrogen electrode (NHE) is displayed against the logarithms of the current density  $j$ .

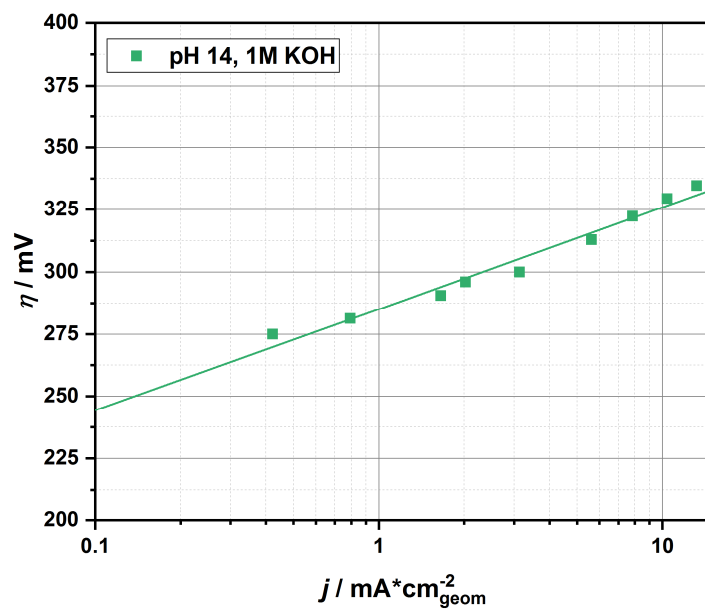


Figure S18. Tafel-plot of MnO<sub>x</sub>/CFP in 1 M KOH-solution (pH 14).

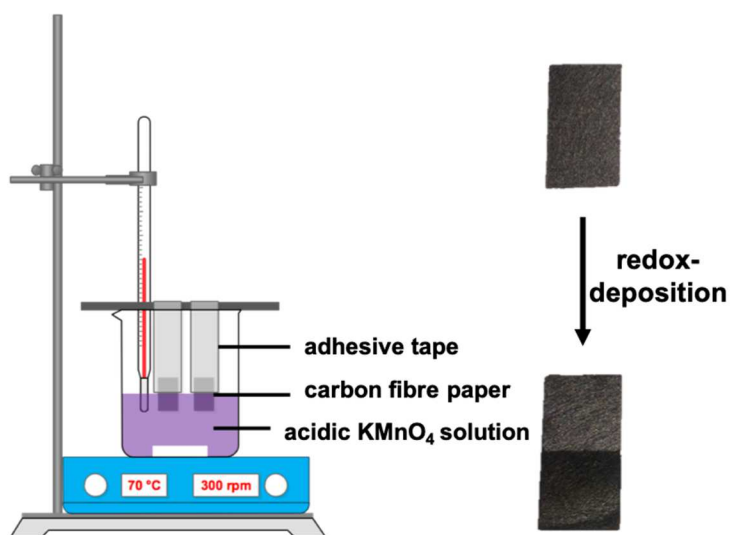


Figure S19. Schematic representation of the electrode preparation process.

## Additional Tables:

**Table S1** EXAFS fit parameters of samples after deposition and drying (60°C) or calcination (400°). Fit R-factor in parentheses.

60°C (R = 15.4)							
shell	type	R [Å]	error	N	error	s [Å]	error
a	O	1.90	0.00	5.0	0.4	0.0593	0.0052
b	Mn	2.87	0.00	5.2	0.6	0.0710	0.0049
c	Mn	3.47	0.01	2.9	0.4	0.050*	
d	O	3.59	0.02	8.0	1.7	0.050*	
e	O	4.78	0.03	5.5	2.9	0.050*	
f	Mn	5.00	0.02	3.2	1.1	0.0612*	
g	Mn	5.54	0.01	8.4	1.5	0.0707*	

400°C (R = 15.9)							
shell	type	R [Å]	error	N	error	s [Å]	error
a	O	1.90	0.00	5.4	0.4	0.0558	0.0047
b	Mn	2.88	0.00	4.5	0.6	0.0714	0.0057
c	Mn	3.45	0.01	3.7	0.5	0.0500*	
d	O	3.57	0.03	4.8	1.7	0.0500*	
e	O	4.75	0.02	7.7	2.6	0.0500*	
f	Mn	5.03	0.01	4.9	1.0	0.0612*	
g	Mn	5.55	0.02	4.1	1.6	0.0707*	

\* value kept constant in the final refinement

**Table S2** EXAFS fit parameters of samples after operation for 24h at different pH. Fit R-factor in parentheses.

pH 2.5 (R = 17.1)							
shell	type	R [Å]	error	N	error	s [Å]	error
a	O	1.90	0.00	6.0*		0.0496	0.0026
b	Mn	2.88	0.00	4.2	0.5	0.0570	0.0052
c	Mn	3.45	0.01	4.9	0.4	0.0500*	
d	O	3.58	0.01	10.1	1.7	0.0500*	
e	O	4.81	0.03	5.7	2.9	0.0500*	
f	Mn	5.04	0.01	4.0	1.1	0.0612*	
g	Mn	5.54	0.02	3.7	1.5	0.0707*	

pH 7 (R = 14.5)							
shell	type	R [Å]	error	N	error	s [Å]	error
a	O	1.90	0.00	5.8	0.4	0.0501	0.0043
b	Mn	2.87	0.00	4.7	0.5	0.0604	0.0047
c	Mn	3.46	0.01	4.0	0.4	0.0500*	
d	O	3.60	0.02	6.6	1.8	0.0500*	
e	O	4.77	0.04	4.1	2.7	0.0500*	
f	Mn	5.02	0.02	3.2	1.0	0.0612*	

g Mn 5.54 0.02 5.8 1.5 0.0707\*

pH 12 (R = 14.6)							
shell	type	R [Å]	error	N	error	s [Å]	error
a	O	1.90	0.00	5.6	0.4	0.0536	0.0045
b	Mn	2.88	0.00	4.6	0.6	0.0687	0.0054
c	Mn	3.45	0.01	2.7	0.4	0.0500*	
d	O	3.59	0.02	6.0	1.7	0.0500*	
e	O	4.72	0.05	3.1	2.7	0.0500*	
f	Mn	4.94	0.02	2.4	1.0	0.0612*	
g	Mn	5.55	0.01	6.2	1.5	0.0707*	

\* value kept constant in the final refinement

## References

- [1] J. Melder, W. L. Kwong, D. Shevela, J. Messinger, P. Kurz, *ChemSusChem* **2017**, *10*, 4491–4502.
- [2] A. L. Ankudinov, B. Ravel, J. J. Rehr, S. D. Conradson, *Phys. Rev. B* **1998**, *58*, 7565–7576.
- [3] J. D. Hanawalt, H. W. Rinn, L. K. Frevel, *Anal. Chem.* **1938**, *10*, 457.
- [4] J. E. Post, D. R. Veblen, *Am. Mineral.* **1990**, *75*, 477–489.